


PEDIATRIC NEUROMONITORING

# Noninvasive Neuromonitoring Modalities in Children Part I: Pupillometry, Near-Infrared Spectroscopy, and Transcranial Doppler Ultrasonography



Marlina E. Lovett<sup>1</sup>, Jennifer M. MacDonald<sup>1</sup>, Marina Mir<sup>2</sup>, Suman Ghosh<sup>3</sup>, Nicole F. O'Brien<sup>1†</sup> and Kerri L. LaRovere<sup>4\*†</sup> 

© 2023 Springer Science+Business Media, LLC, part of Springer Nature and Neurocritical Care Society

## Abstract

**Background:** Noninvasive neuromonitoring in critically ill children includes multiple modalities that all intend to improve our understanding of acute and ongoing brain injury.

**Methods:** In this article, we review basic methods and devices, applications in clinical care and research, and explore potential future directions for three noninvasive neuromonitoring modalities in the pediatric intensive care unit: automated pupillometry, near-infrared spectroscopy, and transcranial Doppler ultrasonography.

**Results:** All three technologies are noninvasive, portable, and easily repeatable to allow for serial measurements and trending of data over time. However, a paucity of high-quality data supporting the clinical utility of any of these technologies in critically ill children is currently a major limitation to their widespread application in the pediatric intensive care unit.

**Conclusions:** Future prospective multicenter work addressing major knowledge gaps is necessary to advance the field of pediatric noninvasive neuromonitoring.

**Keywords:** Pediatric neurocritical care, Neuromonitoring, Pupillometry, Near-infrared spectroscopy, Transcranial Doppler ultrasonography

## Introduction

Brain injury is common in pediatric critical care as a result of either a primary neurological or neurosurgical process, secondary brain injury or as a consequence of systemic disease. The ability to identify children at risk of neurologic injury and detect early signs of neurologic dysfunction is key to providing good critical care.

Pediatric neuromonitoring has traditionally focused on serial neurologic examinations, electroencephalography (EEG), and neuroimaging. Similar to adult neurocritical care, there is an emerging interest in other noninvasive neuromonitoring modalities, particularly automated pupillometry, near-infrared spectroscopy (NIRS), and transcranial Doppler (TCD) ultrasonography. These technologies may provide additional insights into important physiological changes, improve early recognition of acute neurologic deterioration, and help guide management in a meaningful way that improves patient outcomes [1, 2]. In this article, we aim to review pupillometry, NIRS, and TCD ultrasonography in the pediatric intensive care unit (PICU) setting. For each technology, we will discuss the

\*Correspondence: kerri.larovere@childrens.harvard.edu

†Nicole F. O'Brien and Kerri L. LaRovere have contributed equally to this work.

<sup>4</sup> Department of Neurology, Boston Children's Hospital and Harvard Medical School, Boston, MA, USA

Full list of author information is available at the end of the article

basic methods and available devices, use in clinical care and research, and limitations and future directions, realizing that normative data for the PICU population and standardized protocols, data reporting, and interpretation are needed for their safe and effective use in critically ill children.

### Pupillometry

The pupillary light reflex (PLR) is a complex physiologic process involving the sympathetic and parasympathetic nervous system. When light is shined into the eye, retinal photoreceptors are activated via the optic nerve. The optic nerve traverses the optic chiasm, where nerves from the nasal retina cross to the contralateral side and nerves from the temporal retina continue ipsilaterally [3]. After exiting the optic tract, they synapse within the pretectal area of the midbrain. Axons then travel from the pretectal area bilaterally and synapse at both Edinger–Westphal nuclei. The parasympathetic fibers travel via the oculomotor nerves to synapse at the ciliary ganglion and ultimately innervate the iris sphincter, resulting in pupillary constriction [3–5]. In contrast to the parasympathetic nervous system, the sympathetic nervous system is responsible for pupillary dilation. Lesions at any point along these pathways, therefore, may impact the pupillary examination. Pupil size or PLR may be confounded by a variety of medications, alcohol, delirium, and acute brain injury itself [6, 7]. Medications that may impact the static or dynamic evaluation of the pupil include but are not limited to atropine, barbiturates, diphenhydramine, naloxone, opioids, propofol, and selective serotonin reuptake inhibitors [4].

Pupillary assessment is a key component of the neurologic examination of any critically ill child that may be performed qualitatively or quantitatively. Traditionally, this has been examiner dependent and subjective and would include an estimation of pupillary size and reactivity assessed as “brisk,” “sluggish,” or “nonreactive.” Prior research has shown that qualitative assessments of pupils using a penlight have the potential to be inaccurate, with limited interrater reliability, and may not identify changes in pupillary size or reactivity [8–10]. Automated quantitative pupillometry, on the other hand, has allowed for objective data reporting, evaluation of multiple dynamic components of the PLR, and digital visualization of trends that may signify acute neurologic dysfunction.

### Pupillometer Methods and Devices

Although there are a variety of pupillometers reported in the literature, there are two main companies that manufacture devices applicable to the intensivist. Until recently, NeurOptics was the only manufacturer available in the United States. However, as of March 2022, the


pupillometer made by ID Med is now available (Table 1). Handheld pupillometers have their own light source, a self-contained digital camera, and a liquid crystal display screen. The pupillometers made by these two manufacturers have a 510 K US Food and Drug Administration (FDA) exemption and are available in both the United States and Europe. As with any commercial device, individual pupillometer parameters and results may vary across manufacturers. An adult study comparing two commercially available pupillometers (NeurOptics NPi-200 and the NeuroLight Aligscan) showed significant correlation for pupil size and constriction velocity but no correlation for pupillary latency [11].

When using the pupillometer, the examination begins with a flash of light of fixed intensity and duration that stimulates the PLR [14]. Infrared light rays are used to illuminate the eye, and images are acquired by the digital camera [15]. As an example, the NeurOptics NPi-200 captures 90 images in a 3-s period (NeurOptics.com). The results are immediately displayed on the screen and can be trended over time. As such, its use has been associated with reduced nursing assessment time when the pupillometer synchronizes with the electronic medical record (penlight examination: 96 s versus 37 s with the pupillometer) [16].

Automated pupillometry allows for quantitative measurement of multiple variables that cannot be quantified with the human eye. Measured variables vary based on the manufacturer but often include static and dynamic parameters that may be age related and impacted by environmental light conditions (Table 2) [4, 14]. For example, in a study of 90 children aged 1 to 18 years old in ambient light, the mean maximum pupil size was 4.11 mm, the mean minimum size was 2.65 mm, the mean constriction velocity was 2.34 mm/s, the mean dilation velocity was 2.2 mm/s, and the mean pupillary size reduction was 36% following light stimulus [12]. The authors noted larger pupils in children aged 2 to 6 years old, which may be related to myelination [12]. In contrast, under scotopic light conditions, 101 children had a mean resting pupil diameter of  $6.6 \pm 0.74$  mm, a mean minimum size of  $4.7 \pm 0.77$  mm, a mean constriction velocity of  $3.7 \pm 0.744$  mm/s, a mean dilation velocity of  $0.88 \pm 0.25$  mm/s, and a mean pupillary size reduction of  $30\% \pm 6.2\%$  [13].

NeurOptics pupillometers employ a proprietary algorithm to quantify pupillary reactivity called the Neurological Pupil Index (NPi), first introduced in 2011 [14, 17]. The NPi incorporates multiple PLR variables, including size, latency, constriction velocity, and dilation velocity [14]. Each individual variable is compared against the mean reference value of healthy individuals and the difference is standardized to the standard deviation, resulting in a z-score that becomes the NPi [14]. The NPi is

**Table 1 Commercially available handheld pupillometers reported in the ICU literature**

Manufacturer	Models (currently available)	Pros/cons
ID MED (Marseille, France) Idmed.fr Available in Europe and the United States	NeuroLight Algiscan 	Uses eyecup to block out ambient light Does not use any disposable contents, eyecups are reusable Quantifies the pupillary light reflex to 0–5% (nonreactive or fixed), 5–20% (abnormal/sluggish), > 20% (normal/brisk) The Algiscan uses pupillometer data to measure the level of analgesia in a proprietary manner called the pupillary pain index
NeuroOptics (Irvine, CA, USA) neurooptics.com Available in Europe and the United States	NPi-200 NPi-300 	Requires each patient to have their own SmartGuard NPi is proprietary Normative data in children reported using the NeuroOptics ForSite pupillometer [12] and NeuroOptics PLR-200TM [13] NeuroOptics makes additional research models that do not employ the NPi algorithm (outside of the scope of this article)

ICU, intensive care unit, NPi, Neurological Pupil Index

**Table 2 Pupillometer variables**

Variable	Unit of measure	Variable explanation
Pupil size	mm	Minimum pupil size (min): size at peak constriction Maximum pupil size (max): size measured at rest
Constriction percentage or percent change	%	(max – min)/max
Latency	s	Time delay between the light stimulus and the onset of pupillary constriction
Constriction velocity	mm/s	Distance of constriction (mm) divided by constriction duration (average)
Maximum constriction velocity	mm/s	Peak value of constriction velocity
Dilation velocity	mm/s	Distance of redilation (mm) divided by the duration of recovery (seconds)

scored from 0 to 5, in which 0 indicates an absent PLR and 5 indicates a “brisk” PLR. Within the adult literature, an  $\text{NPi} \geq 3$  suggests that pupil reactivity falls “within the boundaries of the normative pupil behavior distribution” [14]. An  $\text{NPi} < 3$  has been termed “abnormal.” There are no data in children to indicate which NPi values are cause for concern.

#### Use of Pupillometry in Clinical Care and Research

In adults, pupillometry-derived PLR has been studied in a variety of applications (e.g., screening for neurologic complications, neuroprognostication) and conditions (e.g., traumatic brain injury [TBI], aneurysmal subarachnoid hemorrhage/intracerebral hemorrhage). In adults with traumatic and nontraumatic intracerebral

hemorrhage, an  $\text{NPi} < 3$  was associated with increased intracranial pressure (ICP) (average 30.5 mmHg), whereas an  $\text{NPi} \geq 3$  was associated with normal ICP (average 19.6 mmHg). In a subset of these patients, pupillometry was able to identify changes in pupillary reactivity preceding intracranial hypertension [14]. Findings in adults have also suggested that pupillary constriction velocity  $< 0.6$  mm/second, an  $\text{NPi} < 3$ , and pupil size reduction  $< 10\%$  have been associated with intracranial hypertension [4]. In a small cohort of adults with aneurysmal subarachnoid hemorrhage, an  $\text{NPi} < 3$  was associated with the development of delayed cerebral ischemia [18]. The pupillometer has been reported to aid in neuroprognostication following a variety of acute neurologic conditions [4]. In a study of 103 adults following cardiac arrest, 48-h quantitative PLR percentage reactivity  $\geq 13\%$  distinguished survivors from nonsurvivors (PLR  $< 13\%$  had a 100% positive predictive value for mortality with 100% specificity) [19]. In a multicenter trial of 456 adults following cardiac arrest, an  $\text{NPi} \leq 2$  at any time between days 1 and 3 was associated with unfavorable outcome with 32% sensitivity, 100% specificity, and a 100% positive predictive value, exceeding performance metrics of the manual pupillary examination [20].

In children, the pupillometer has been used in TBI, stroke, central nervous system infections or malignancies, seizures, encephalopathy, septic shock, cerebral edema, and extracorporeal membrane oxygenation [1]. In a recent survey of neuromonitoring practices in 52 PICUs, 17 (33%) intensive care units reported using pupillometry [1]. Pupillometry use was guided by institutional protocols (ten hospitals, 59%), a pediatric intensivist (ten hospitals, 59%), the neurosurgical team (four hospitals, 24%), and/or the neurology team (six hospitals, 35%). In this survey, the pupillometer was most frequently used in children with severe hypoxic-ischemic brain injury following cardiac arrest (29%), severe TBI (27%), and cerebral edema with no clear underlying etiology (25%) [1]. There are no known specific thresholds or values derived from pupillometry in children that have been clearly associated with unfavorable patient outcomes or acute change in management, and trends in data may be helpful. Freeman and colleagues [21] attempted to evaluate whether abnormal pupillary measurements would precede increases in ICP in a cohort of 28 children with acute brain injury and ICP monitors. When ICP was  $< 20$  mmHg ( $n = 856$  measurements), right and left  $\text{NPis}$  were 4.4 and 4.4, whereas when ICP was  $\geq 20$  mmHg ( $n = 315$  measurements), the right  $\text{NPi}$  was 3.4 and the left  $\text{NPi}$  was 3.3. There was an inverse correlation with  $\text{NPi}$ , pupillary size, constriction velocity, maximum constriction velocity, and dilation velocity with ICP but no significant correlation with

latency [21]. These authors suggested that individual measured parameters that contribute to the  $\text{NPi}$  may better correlate with ICP than the absolute  $\text{NPi}$  score itself [21]. Although normative data exist for a number of components of the PLR in healthy children using the pupillometer [12, 13], it is unclear whether there is a specific  $\text{NPi}$  cutoff in children that indicates “normal” or “abnormal” PLR and what defines a clinically meaningful change in the  $\text{NPi}$  for each manufacturer.

The current evidence base regarding the use of automated pupillometry in critically ill children is limited. The World Brain Death Project suggests using a pupillometer during the clinical examination for determination of brain death [22]. Outside of this recommendation, there are no other societal guidelines or consensus statements with clear recommendations as to which critically ill children would benefit from the use of automated pupillometry as a routine portion of their care. Therefore, the use of automated pupillometry is likely best integrated based on individual institutional standards for neurologic examinations of the critically ill child as recommended by a pediatric intensivist, neurologist, or neurosurgeon.

#### Pupillometry Limitations and Future Directions

Automated pupillometry has the potential to impact clinical care for the critically ill child. The objective data obtained from the pupillometer may allow for early detection of impending neurologic deterioration, may serve as a marker that one could trend pre-intervention and post-intervention, may assist in the noninvasive detection of intracranial hypertension, and may have utility in aiding in neuroprognostication. Prospective studies are needed to better understand these and other clinical applications for pupillometry in the PICU and how pupillometry may impact clinical decision-making at the bedside. Standardized data reporting and interpretation that does not focus solely on analyzing proprietary algorithms is needed to be most generalizable to the global field. Performance metrics of pupillometry for outcomes of interest also need to be better understood.

#### NIRS

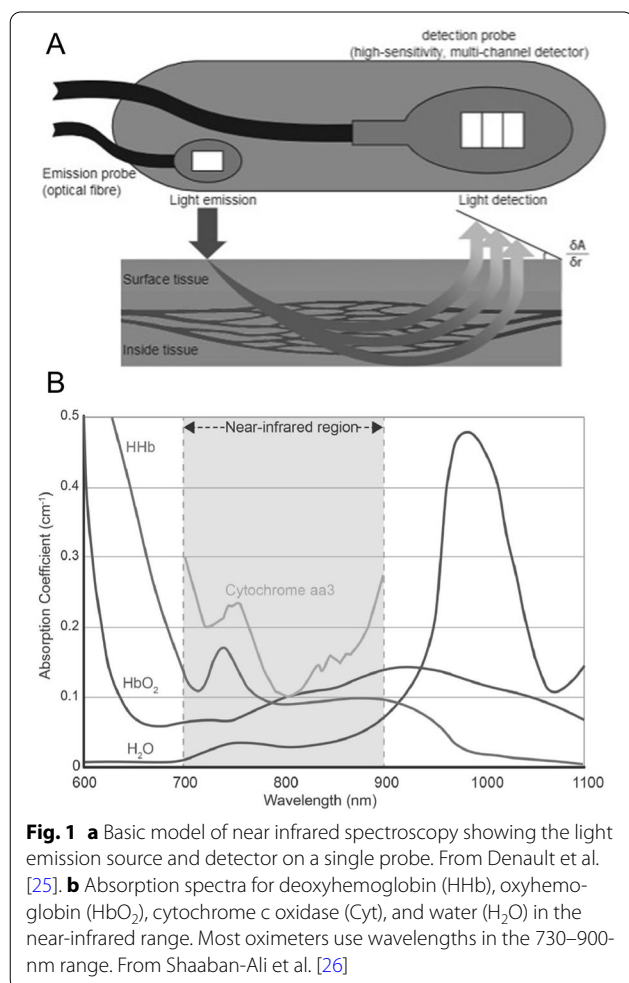
Optimizing oxygen delivery to various tissues is a key goal in critical care. The noninvasive measurement of blood oxygenation via pulse oximetry revolutionized patient management in the 1970s because it gave clinicians a tool to measure systemic oxygen levels, to recognize hypoxemia before it was otherwise obvious, and to respond with changes in treatment [23]. Around the same time in 1977, NIRS was described as a noninvasive tool to detect the oxygenation state of living tissue by Jobsis [24]. Since then, the role for NIRS has been a

**Table 3 FDA-approved NIRS devices commercially available in the United States**

Company	Instrument name	Sensors available	Wavelengths	Additional information
Nonin Medical Inc	SenSmart	Adult and pediatric	730, 760, 810, 880 nm	
Edwards Lifesciences	Fore-Sight	Adult, pediatric/medium (> 3 kg), infant/small (< 8 kg)	5 total: 690, 778, 800, 850 nm plus one additional on adult probe, 685 nm on pediatric/infant probe	Reports compensation for melanin [27] Small probe is available without adhesive
Medtronic	INVOS	Adult (> 40 kg), infant (< 5 kg)	730, 810 nm	
Mesepere Life Sciences	NeurOs—Cerebral Oximetry	Adult		Single use and reusable probes available Provides blood volume index
Masimo	O3 Regional Oximetry	Adult (> 40 kg), pediatric (5–40 kg), infant (< 10 kg)	730, 760, 810, 880 nm	

Each uses similar technology but differs in the wavelengths used and components of proprietary computational algorithms. Other devices are available in other countries and for research use

FDA, US Food and Drug Administration, NIRS, near-infrared spectroscopy



focus of research, resulting in thousands of publications and review articles, and its use has been integrated into clinical practice in various ways, importantly to assess cerebral regional oxygenation (rSO<sub>2</sub>).

### NIRS Methods and Devices

NIRS is a reasonably priced, portable, relatively small, noninvasive monitor that does not require ionizing radiation and can be quickly applied at the bedside without the need for ongoing hands-on operation. A list of FDA-approved NIRS devices that are commercially available in the United States is shown in Table 3. A probe, which contains both the light emission source and the detection sensor, is applied to the area of interest (e.g., forehead for cerebral monitoring), and data are transmitted to a processor with a display (Fig. 1a). Most machines have neonatal or pediatric probes, which differ from adult probes by the size of the footprint and different depth of light penetration to compensate for the thinner skull of infants and children. Near-infrared light of various wavelengths is emitted from the probe, passes through skin and bone, and diffuses through the tissue, where it encounters hemoglobin in its different states of oxygenation in the arteries, veins, and capillaries in a manner that is not flow dependent. Importantly, deoxyhemoglobin and oxyhemoglobin absorb light at different wavelengths (Fig. 1b). Reflected light is measured by the detection sensor, and these data are processed through a series of complex mathematical transformations with a basis in the modified Beer–Lambert law to provide information about tissue oxygenation. A typically proprietary algorithm that includes compensation for the light penetration depth and other factors is used by each device to provide a regional cerebral oxygen saturation (rSO<sub>2</sub>), which is expressed as a percentage (oxyhemoglobin/total hemoglobin × 100) displayed on the monitor, along with the trend over time.

There are no well-validated normative thresholds, and there is no true gold standard for rSO<sub>2</sub>, making the trend in data likely more valuable than any individual point in time. However, rSO<sub>2</sub> obtained using NIRS has been shown to correlate with jugular bulb saturation

(the closest to a gold standard for the measurement of the balance between cerebral oxygen delivery and use that exists) [28–34]. There is also variability between each NIRS machine because of variations in probe size, depth of beam penetration, signal processing, and data analysis. Although there is no FDA standard for accuracy as there is with pulse oximetry, for example, which must have an accuracy root mean square within 2–3% of arterial blood gas values, comparative studies of several commercially available systems have shown that they are generally equivalent within  $\pm 10\%$  in both real-world and laboratory settings [35–39]. Furthermore, the calculation of rSO<sub>2</sub> requires assumptions that may not be true in all clinical scenarios. For example, most systems assume around 10% intracapillary/20% intraarterial/70% intravenous blood volume distribution, and calculations are weighted appropriately. However, there may be individual variability leading to inaccurate results for that specific patient [40]. There are also physiologic or pathophysiologic changes in the arterial/venous ratio that occur, which may lead to inaccuracy of cerebral oximetry [41]. For example, Schober et al. [42] compared the difference between measured rSO<sub>2</sub> and that calculated from jugular venous and radial arterial hemoglobin saturations using the manufacturer-provided ratios in healthy volunteers over a range of fraction of inspired oxygen (FiO<sub>2</sub>) and two partial pressure of carbon dioxide in arterial blood (PaCO<sub>2</sub>) levels. They showed that acute hypocapnia, which presumably changes the arterial/venous ratio, led to an overestimate of rSO<sub>2</sub>, and the difference was exacerbated with lower FiO<sub>2</sub> [42]. Additionally, it is assumed that most of the data collected by the probe come from the brain, with minimal contribution from the skin and tissues. However, this may not always be the case; for example, different forehead shapes, larger sinuses, tissue edema, or scarring may create artifact or interference with the probe or add a more than minimal contribution to the rSO<sub>2</sub> calculation [43]. Because of these limitations, NIRS-derived rSO<sub>2</sub> has variability both between patients and within the same patient, making quantitative analysis less valuable than trend monitoring [36, 44]. Although studies using different machines in different populations have generated different normative data, a baseline rSO<sub>2</sub> of around 55–75% in adults and children without cyanotic heart disease is commonly accepted [45–48]. Kurth et al. [49] described the effect of hypoxia on the brain in a piglet model and showed that impairment occurred in a graded fashion and established general thresholds for concern (Fig. 2). Slowing in the EEG and increased brain tissue lactate levels were seen at a NIRS rSO<sub>2</sub> of 40–45%, and this progressed to flat EEG results at a NIRS value around 30% [49].

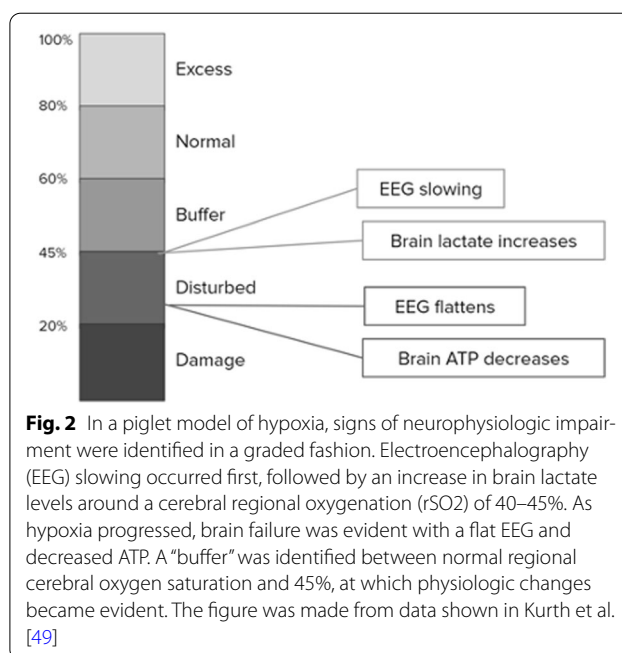


**Fig. 2** In a piglet model of hypoxia, signs of neurophysiologic impairment were identified in a graded fashion. Electroencephalography (EEG) slowing occurred first, followed by an increase in brain lactate levels around a cerebral regional oxygenation (rSO<sub>2</sub>) of 40–45%. As hypoxia progressed, brain failure was evident with a flat EEG and decreased ATP. A “buffer” was identified between normal regional cerebral oxygen saturation and 45%, at which physiologic changes became evident. The figure was made from data shown in Kurth et al. [49]

#### Use of NIRS in Clinical Care and Research

The body of literature evaluating the use of cerebral NIRS in a variety of neonatal and pediatric conditions in the intensive care unit suggests that it may be a useful adjunct with multimodal monitoring, but the impact on patient management and outcomes from NIRS alone remains unclear. In a systematic review from the Cochrane library that examined the use of NIRS in premature infants born 12 weeks early and outcomes, including mortality and later neurologic development, one randomized clinical trial was included involving 166 premature infants randomized to continuous cerebral NIRS monitoring until 72 h after birth and appropriate interventions if NIRS was out of normal range according to a guideline versus conventional monitoring with blinded NIRS. The trial was powered, however, to detect a difference in cerebral oxygenation and not morbidities or mortality. No consistent effects of NIRS along with a guideline on the assessed clinical outcomes were seen. Validity was hampered by a small sample, lack of blinding, lack of power, and indirectness of outcomes [50]. Assessment of cerebral autoregulation using NIRS in the neonatal population with hypoxic-ischemic encephalopathy is beyond the scope of this review. Another systematic review on the use of cerebral NIRS in congenital heart disease reviewed available data from 47 case series, four randomized trials, and three retrospective studies. The data suggested that this literature failed to find an association between the use of NIRS and neurologic outcomes, and the authors concluded that this limits the support for widespread

implementation [51]. A recent survey, however, of 52 North American PICUs showed that 87% of respondents reported using NIRS in clinical care at their institution. Patients were chosen for monitoring primarily at the choice of the PICU attending (89%) or based on institutional protocol (56%), and primary reasons for monitoring included ECMO (69%), severe hypoxic-ischemic brain injury after cardiac arrest (56%), and severe TBI (48%) [1]. This study does not provide information on frequency of usage or how NIRS was used, and it does not represent usage outside of North America.

In pediatric TBI, small studies support the use of NIRS [52–55]. In a small pilot study by Kampfl et al. [52] involving eight patients with ICP monitors post head injury, rSO<sub>2</sub> was lower in the high ICP group (>25 mmHg) than in the low ICP group (<25 mmHg). Another study by Kirkpatrick et al. [53] of 14 ventilated patients with closed head injury also showed that NIRS changes correlated with changes in cerebral perfusion pressure identified by multimodal monitoring 97% of the time. Studies by Zuluaga et al. and Lang et al. showed that rSO<sub>2</sub> trended lower with increased ICP in patients with brain tumors, trauma, and hydrocephalus pre- and post cerebrospinal fluid (CSF) diversion [54, 55].

The small size and portability of NIRS makes it feasible to use in a prehospital setting, and it has been successfully studied by noncivilian groups as a tool to identify traumatic intracranial hemorrhage in the field [56–58]. Pediatric research teams have looked at the use of NIRS for detection of intracranial hemorrhage in children because of these promising results. Studies by Salonia et al., Bressan et al., Lewartowska-Nyga et al., and Kirschen et al. each found that the Infrscan, a handheld NIRS device, identified intracranial hemorrhage that was confirmed by head computed tomography with reasonable sensitivity and specificity [59–62]. This device does not use rSO<sub>2</sub> but rather determines differences in the optical density, which is higher in areas of hemorrhage because of increased hemoglobin levels and therefore more absorbent of NIRS light. These studies each show that the handheld NIRS device has a high negative predictive value in their cohorts, suggesting it could act in an adjunctive role with current clinical decision rules to predict risk of intracranial hematoma in children with head trauma. Further research in large cohorts with a focus on effectiveness will be valuable in clarifying the role for this technology, which has the potential to decrease radiation exposure via computed tomography scans and shorten length of observation for patients who may have previously required these interventions.

In post-cardiac-arrest monitoring, studies in adults have suggested a role for cerebral NIRS during cardiac arrest, with higher rSO<sub>2</sub> values correlating with return

of spontaneous circulation (ROSC) and neurologically favorable survival to hospital discharge [63–65]. Several small case series have described use of NIRS in pediatric cardiac arrest [66–68]. A small prospective study by Francoeur et al. [69] in 2022 showed that NIRS placement during pediatric in-hospital cardiac arrest was feasible and that the median rSO<sub>2</sub> was higher for events with ROSC than those with no ROSC, but there was no association between rSO<sub>2</sub> and survival to discharge. As the field of cardiac arrest research focuses on goal-directed cardiopulmonary resuscitation, cerebral NIRS can noninvasively assess rapid changes in cerebral oxygenation, which may correlate with more effective cardiopulmonary resuscitation and improved neurologic outcomes, but larger studies are required to determine its role in this clinical scenario.

Lastly, small pediatric studies suggest that use of NIRS-derived optimal blood pressure determination is feasible post cardiac arrest [70, 71]. Kirschen et al. [72] showed that a larger amount of time with the mean arterial pressure (MAP) below the NIRS-derived optimal MAP (MAP<sub>opt</sub>) during the first 24 h after cardiac arrest correlated with unfavorable outcomes (Pediatric Cerebral Performance Categorization  $\geq 3$  with  $\geq 1$  change from baseline at the time of hospital discharge). Similarly, Lee et al. [73] showed that a larger time with MAP below MAP<sub>opt</sub> or a larger deviation below MAP<sub>opt</sub> was associated with new tracheostomy or gastrostomy, brain death, or withdrawal of technological support for neurologic futility. This is an area that requires further research to clarify the role for NIRS in the care of children post arrest.

As highlighted previously, there is a large breadth of studies using NIRS in critically ill pediatric patients. Although there is insufficient evidence to support formal guidelines surrounding its use, there is also no evidence showing harm through the use of this noninvasive device. When the device can be placed around other clinically indicated equipment (e.g., EEG leads), NIRS could be used as a component of multimodality monitoring of patients with neurologic injury [51]. As with other noninvasive monitoring devices, trends in NIRS data may be the most clinically useful. To use cerebral NIRS clinically in any scenario, it is important to remember that cerebral rSO<sub>2</sub> is a result of cerebral tissue oxygen supply (a factor of cerebral blood flow and arterial O<sub>2</sub> content) minus the demand (Fig. 3a). There are many physiologic alterations that can affect this number, and different interventions may be required. For example, low rSO<sub>2</sub> may be due to low oxygen delivery from decreased cardiac output and hypotension. In this case, recognizing and treating the hypotension should improve the rSO<sub>2</sub>. Alternatively, if cerebral oxygen demand is high because of seizures,

(See figure on next page.)

**Fig. 3** **a** Examples of physiologic factors that impact cerebral oxygenation. **b** An example of a management algorithm using cerebral near-infrared spectroscopy (NIRS) data during cardiac surgery as shown by Trafidlo et al. [75]. rSO<sub>2</sub>, regional cerebral oxygen saturation, HgB, hemoglobin, CBF, cerebral blood flow, SpO<sub>2</sub>, oxygen saturation, CPP, cerebral perfusion pressure, MAP, mean arterial blood pressure, ICP, intracranial pressure, PaO<sub>2</sub>, partial pressure of oxygen in arterial blood, PaCO<sub>2</sub>, partial pressure of carbon dioxide in arterial blood, SvO<sub>2</sub>, venous oxygen saturation, CMRO<sub>2</sub>, cerebral metabolic rate of oxygenation consumption

antiseizure medication is required to normalize the rSO<sub>2</sub>. Although there are no accepted protocols or guidelines for when to use NIRS and how to interpret the data in the PICU population that have been shown to result in improved patient-specific outcomes, algorithms have been created by various institutions to help clinicians use the information obtained from NIRS in addition to other physiologic parameters to modify clinical care (Fig. 3b) [74, 75]. Further research is needed to validate these algorithms in the PICU for NIRS to be safely and effectively incorporated into clinical care.

#### NIRS Limitations and future directions

Cerebral NIRS monitoring has several limitations, some of which are related to the physics behind the machine's function and the physiology of the brain in normal and pathologic states. As discussed previously, the lack of validated normative thresholds may make a trend more meaningful than individual data points. Additionally, the data obtained are subject to physiologic or pathophysiologic changes of noncerebral origin. A small laboratory-based study evaluated the impact of varying levels of skin pigmentation and melanin on NIRS oxygenation readings and found that as the level of pigmentation increased, the reported saturation decreased [76]. Clinically, this was assessed by Sun et al. [77] in a retrospective registry study in which they found that self-identified African American patients had a lower rSO<sub>2</sub> when compared with White patients. This is a potential source of bias that must be addressed in research going forward, and clinicians must be aware of this limitation in the interim. NIRS monitors measure regional brain tissue oxygenation in the frontal regions, and therefore any change seen reflects changes in this part of the brain only. Measurements also reflect only the tissue oxygenation in the outer cortex because beams are unable to reach deeper segments of the brain. Additionally, a local change may occur in a nonfrontal brain region that would not be detected by the NIRS monitor in the frontal region. Logistical challenges exist for smaller children who have smaller forehead sizes, and the probes may not fit well or may interfere with other forms of monitoring (e.g., EEG). Interference may also arise from other equipment at the bedside, such as respiratory or cardiac oscillations. Lastly, a tightly adherent probe is necessary for appropriate data collection,

and frequent readjustment may be necessary because of probe dislodgement.

To further highlight the limitations and challenges of NIRS, we can look to the adult literature, in which recent studies have directly compared NIRS monitoring with invasive brain tissue oxygen (PbtO<sub>2</sub>) monitoring and found various levels of correlation in various pathologies. de Courson et al. [78] found no correlation between the two methods in a cohort of 51 patients with non-traumatic subarachnoid hemorrhage. These data were collected manually each hour, and there was no global correlation over time. When looking at patients with severe TBI, presumably a more global injury, studies have shown variable but present correlation between invasive and NIRS monitoring [79–81]. The differential information obtained from invasive and noninvasive monitoring may be because invasive PbtO<sub>2</sub> monitors assess oxygen concentration of the interstitial tissue in the deeper white matter, whereas NIRS measures oxygen in intravascular space closer to the brain surface [82]. These two monitoring sources may have differential baseline values from different parts of brain tissue. Additionally, the sampled areas may also be affected differently by brain pathology; for example, if the invasive monitor is placed into injured tissue, local microvascular injury may lead to decreased diffusion of O<sub>2</sub> that is not occurring globally in the whole brain monitored by NIRS. Together with other forms of multimodal neuromonitoring, invasive PbtO<sub>2</sub> and NIRS monitoring may be complementary to each other, and the utility of each may be different depending on the type of injury.

Large prospective studies with patient-centered outcomes are needed to better understand the role of NIRS as a component of multimodal neuromonitoring in the PICU. Uniform data collection and reporting standards are needed to compare results across studies and sites, and adjustment for variation in proprietary algorithms is needed.

#### TCD Ultrasonography

Transcranial Doppler was introduced in the early 1980s by Dr. Aaslid, who described the ability of this device to measure cerebral blood flow velocity (CBFV) in the basal large cerebral arteries around the Circle of Willis through an intact skull bone using low-frequency pulsed Doppler



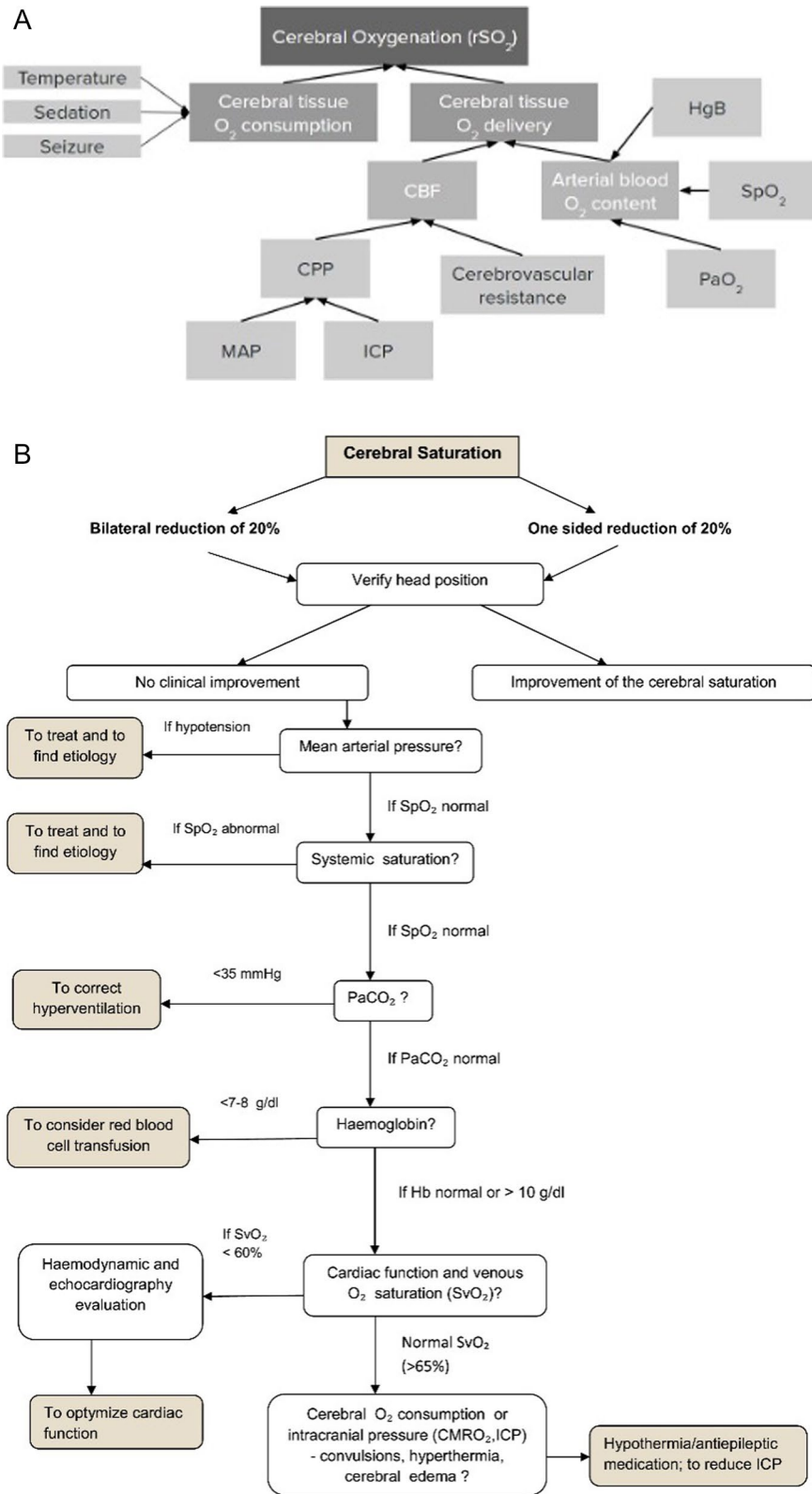


**Fig. 3** (See legend on previous page.)

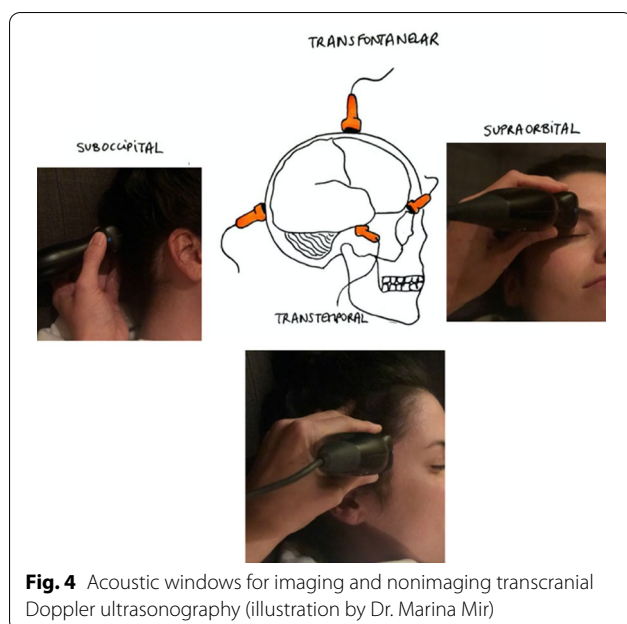


**Fig. 4** Acoustic windows for imaging and nonimaging transcranial Doppler ultrasonography (illustration by Dr. Marina Mir)

ultrasound [83]. Because cerebral hemodynamic information from TCD is obtained in real-time at the bedside, and a single study can be done rapidly and repeated, TCD is not only a diagnostic tool but also an ideal tool for

neuromonitoring [84]. Indeed, technological advances have improved TCD technology since its inception, leading to a broad range of potential applications in the PICU setting. TCD has been used in many different pediatric and adult patient populations in the intensive care unit and perioperative setting in the qualitative assessment of raised ICP, cerebral circulatory arrest, and high-intensity transient signals/microemboli as well as in the quantitative assessment of cerebral vasospasm, cerebral pressure autoregulation, and cerebral vasomotor reactivity [85].

#### TCD Methods and Devices

A low-frequency ultrasound probe (1–3 MHz) is placed over an acoustic window, which is a region of the skull that is thin and permits penetration of the ultrasound. The most common acoustic windows are transtemporal, suboccipital, and orbital (Fig. 4, Table 4). In infants under 12 months of age, the transfontanelle window can also be used. The vessel segments around the Circle of Willis insonated using TCD are shown in Fig. 5. TCD studies may be obtained using imaging (transcranial color-coded duplex ultrasonography [TCCD]) or nonimaging TCD devices depending on local availability and user preference (Table 5). Both modalities use pulsed wave Doppler to generate cerebral hemodynamic information through waveform analysis (Fig. 6). The conventional approach

**Table 4** Insonated vessels in each acoustic window [88–90, 103]

Window	Modality	Vessel segment
Transtemporal	Imaging (TCCD) and nonimaging (TCD)	Middle cerebral artery Anterior cerebral artery Posterior cerebral artery Internal carotid artery terminus
Transfontanelle (anterior fontanelle)	Imaging (TCCD)	Internal carotid artery Ophthalmic artery Basilar artery <i>Anterior cerebral artery and its branches:</i> Pericallosal Callosal marginal Medial frontal <i>Middle cerebral artery and its branches:</i> Lenticulostriate Operculo insular Cortical arteries <i>Posterior cerebral artery and its branches:</i> Thalamic Choroidal
Transoccipital	Imaging (TCCD) and nonimaging (TCD)	Vertebral artery Basilar artery
Transorbital	Imaging (TCCD) and nonimaging (TCD)	Ophthalmic artery Internal carotid artery siphon
Submandibular	Imaging (TCCD) and nonimaging (TCD)	Extracranial internal carotid artery
Transfrontal	Imaging (TCCD) and nonimaging (TCD)	Anterior cerebral artery
Posterolateral fontanelle (posterior and mastoid)	Imaging (TCCD) and nonimaging (TCD)	Posterior circulation in neonates and infants

TCCD, transcranial color Doppler, TCD, transcranial Doppler

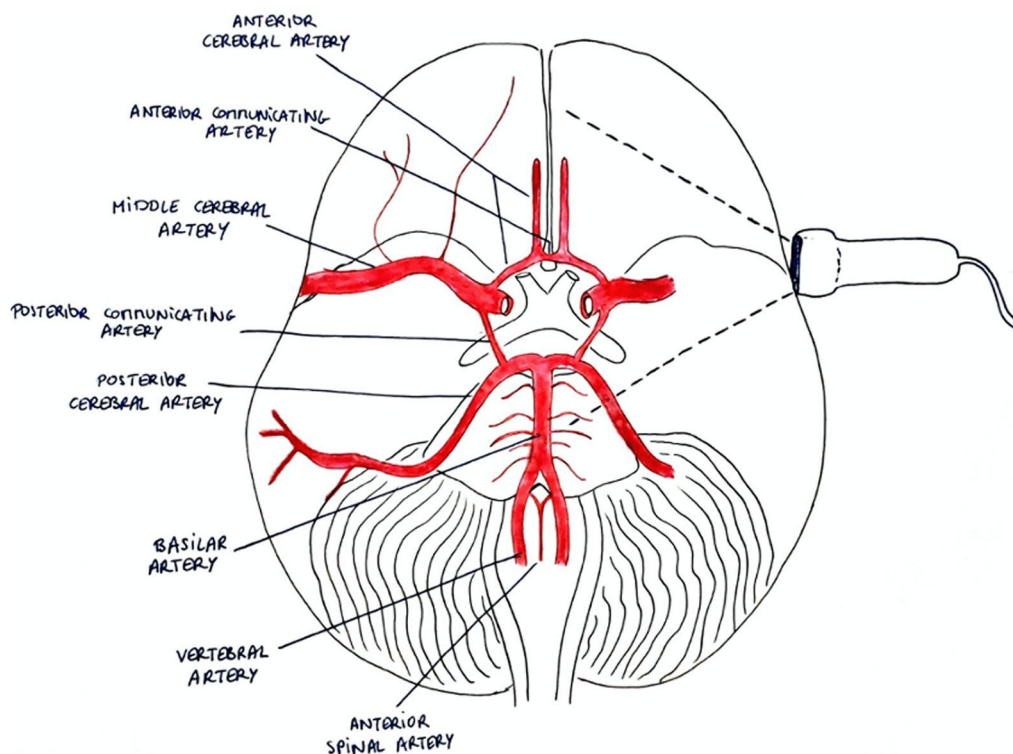


**Fig. 5** Vessel segments around the Circle of Willis that can be insonated with transcranial Doppler ultrasound. Insonation of the large intracranial arteries with the ultrasound probe placed over the transtemporal window is demonstrated in the figure (illustration by Dr. Marina Mir)

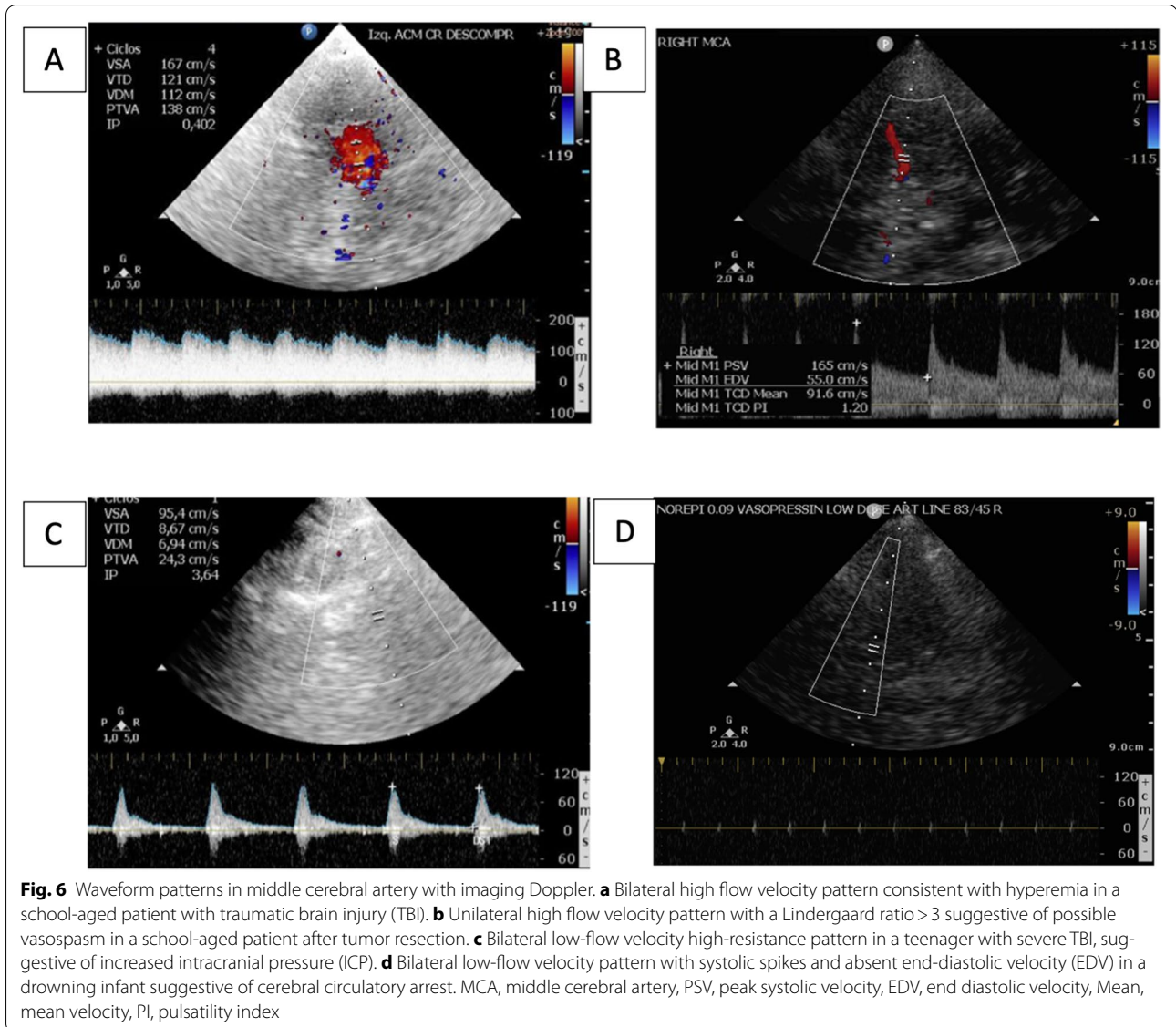
**Table 5** Imaging (TCCD) compared to nonimaging (TCD) devices

Characteristic	TCD	TCCD
Images	Spectral color wave forms	Anatomical images with black and white wave forms
Probe	2-MHz flat probe	2–3.5-MHz phase array probe
Hardware	Dedicated TCD software and hardware	Software package on ultrasound machine
Multichannel monitoring	Yes	No
Angle correction capability	No	Yes
DICOM capable	Some	Yes
Machine size	Small, portable	Large often with cart or carrying case
Upgradable	No	Yes
Learning curve	Moderate	Low

DICOM, Digital Imaging and Communications in Medicine, TCCD, transcranial color-coded duplex ultrasonography, TCD, transcranial Doppler ultrasonography

using nonimaging devices requires vessel identification to occur by knowledge of the typical depth, speed and direction of flow in relation to the probe, waveform morphology, and sound/pitch for each insonated segment. This approach does not require angle correction and assumes a zero angle between the probe and direction of blood flow (angle of insonation). Modern TCD devices have motion (M) Doppler mode, which uses 33 overlapping Doppler samples over 6 cm, which allows the user to visualize the depth at which flow is present and

facilitating localization of the signal [86, 87]. TCCD provides anatomical B-mode images of insonated segments, allowing users to directly visualize the cerebral arteries. The TCCD transducer is a phase array probe operating at frequencies of 2 to 3.5 MHz. The TCCD user can identify landmarks such as the midbrain for orientation to the anterior and posterior circulations using color flow Doppler. CBFV is superimposed on the anatomical images of the blood vessels and flow is color coded with red, indicating flow toward the probe, and blue, indicating flow



away from the probe. Once the vessels are identified, a defined region of measurement called a gate within the B-mode image is identified, from which Doppler shifts are recorded, creating a black and white pulse wave Doppler waveform from the sampled section. Pulse wave Doppler images from gated samples are often displayed alongside the color-coded B-mode image (Fig. 7). TCCD allows the user to visualize both the vessel and segment from which CBFVs are sampled. Angle correction can be applied with imaging devices, but generally this is not done with data acquired from TCCD.

Both TCD modalities measure CBFVs in the large intracerebral arteries around the Circle of Willis and display spectral waveforms on the monitor. Under non-pathologic conditions, cerebral blood flow moves in one

direction within the vessel lumen and demonstrates flow acceleration in systole and stepwise deceleration during diastole. Quantitative variables derived from TCD include peak systolic velocity (PSV), end-diastolic velocity (EDV), and mean flow velocity (MFV) (Fig. 8). Parameters derived from these measurements are the resistive index (RI) and the pulsatility index (PI), which reflect downstream vascular resistance. Of note, cardiac disease states, such as aortic insufficiency or persistent ductus arteriosus, may also influence measurements of vascular resistance.

- $PI = (PSV - EDV) / MFV$ : Normal values for adults are 0.6 to 1.2. Higher PI values indicate higher cerebrovascular resistance downstream from the site of insonation.

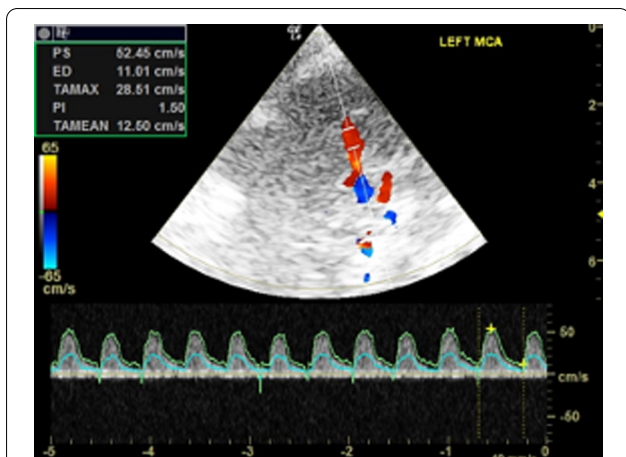


**Fig. 7** Sample image from color duplex transcranial Doppler ultrasound (TCCD). MCA, middle cerebral artery, PS, peak systolic velocity, ED, end diastolic velocity, TAMAX, time-averaged maximum velocity (green envelope tracing), TAMEAN, time-averaged mean velocity (blue envelope tracing)

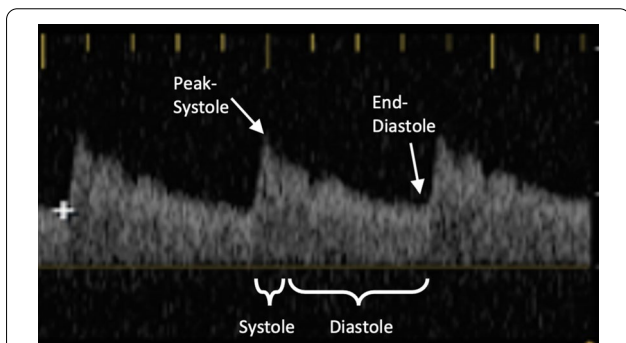


**Fig. 8** Normal transcranial Doppler ultrasound waveform with sharp systolic flow acceleration, stepwise deceleration, and end-diastolic flow observed above the baseline. Additionally, end-diastolic flow velocity values in the cerebral arteries are normally between 20 and 50% of peak systolic flow velocity values

- $RI = (PSV - EDV) / PSV$ : Commonly used in the neonatal population, normal is  $< 0.8$ .

Qualitative information that can be obtained by visual inspection of TCD waveforms includes the following:

- Waveform morphology: Low-resistance waveforms are characterized by sharp systolic upstroke, stepwise deceleration, and robust EDV. High-resistance vascular beds are noted by sharp systolic upstroke, stepwise deceleration, and low EDV [91]. In nonpathologic conditions, the cerebral vascular bed is a low-resistance bed.

- Pattern of flow: High-flow velocity pattern may indicate hyperemia (e.g., due to reperfusion injury following cardiac arrest, infection, hypercapnia) or arterial narrowing (e.g., vasospasm following subarachnoid hemorrhage or tumor resection, or vascular injury in TBI). Low-flow velocity pattern may suggest cerebral hypoperfusion, perfusion limiting increased ICP, or low cardiac output.

The integration of TCD into multimodal neuromonitoring may allow for the evaluation and analysis of model-based indices of cerebrovascular dynamics, including cerebral autoregulation, critical closing pressure, arterial time constant, and compliance of the cerebrovascular bed, among others. Supplemental Table 1 reviews concepts and calculations for model-based indices of cerebral hemodynamics. Noninvasive ICP estimation in children using a circuit model-based algorithm in a coupled analysis with time-synchronized arterial blood pressure waveforms obtained via radial artery catheterization and TCD-derived CBFV measurements may enable continuous, calibration-free, patient-specific ICP estimation in clinical scenarios in which invasive ICP monitoring is impractical [92, 93]. Improving in-depth knowledge of these factors calculated and observed in real time at the bedside may facilitate management of cerebrovascular pathologies.

It will be important to standardize the performance and reporting of TCD data to minimize interoperator variability [93–95] and reduce variability in results within and between centers. In 2020, a multidisciplinary group of TCD experts undertook a modified Delphi study and developed 34 recommendations in four domains for TCD practice in pediatric critical care (indication and request for examination standards, technical performance standards, data interpretation standards, and data reporting standards). A standard basic TCD protocol and a reporting worksheet were created based on the consensus statements [94]. If incorporated into multimodal monitoring, standardization of TCD data elements and reporting processes may also inform clinical decision-making [96].

#### Use of TCD Ultrasonography in Clinical Care and Research

Despite the lack of high-quality evidence supporting the utility of TCD in the PICU, the use of TCD has been explored in a variety of clinical disease states in critically ill children. A recent survey of 27 centers found that TCD was most commonly used in the evaluation and management of children in the PICU with intracranial/subarachnoid hemorrhage (20 hospitals), arterial ischemic stroke (14 hospitals), and TBI (10 hospitals) [97]. In these and other conditions, 74% (20 of 27) of the respondents reported that TCD was used to inform clinical care, such

as when to perform neuroimaging, when to guide cerebral perfusion pressure management, and/or when to consider a surgical intervention. A review of the current pediatric research literature on TCD in pediatric critical care can be found in Supplemental Table 2. The majority of these studies investigated the use of TCD as a diagnostic tool. Investigations of the role of TCD as a neuromonitoring tool included its use in noninvasive estimation of ICP [93], its use in guiding resuscitation after cardiac arrest [98], and its use in guiding cerebral perfusion pressure augmentation in high-risk children with central nervous system infection [99].

To date, the use of TCD remains investigational in children, with the exception of those with sickle cell disease. For example, the use of TCD for ICP estimation is hypothesis-generating because research to date has not yet demonstrated in children how model-based estimation of ICP using TCD would perform when ICP is elevated above the threshold for treatment. At the present time, clear clinical indications for when TCD should be used in critically ill children remain unknown. In these authors' experiences, TCD is used on an ad hoc basis when specific questions around neurovascular pathology arise that cannot be answered with traditional imaging techniques. Furthermore, societal-based guidelines in adults or children that delineate who should perform TCD do not exist. Future research directions should focus on guidelines for specific clinical applications for TCD in pediatric critical care, who should perform TCD (e.g., radiologists, sonographers and/or others), and which data elements are important to collect and how often.

### TCD Limitations and Future Directions

TCD is operator dependent, and from the perspective of the clinician, mastery in the ICU setting requires expertise in the interpretation of findings in the context of underlying clinical conditions and treatments commonly encountered in the ICU. TCD-derived CBFV measurements are a surrogate measure of cerebral blood flow as long as vessel diameter and blood viscosity remain constant (flow equals velocity times area) [100]. Recently it has been reported in adults with delayed neurologic deterioration after subarachnoid hemorrhage that TCD-derived CBFVs in the large cerebral arteries were not reflective of cerebral perfusion disturbances in the downstream smaller arteries by positron emission tomography scan [101], potentially challenging the concept of cerebral vasospasm as a factor in this outcome. More work may be needed to better extrapolate when such circumstances may occur in children. There is ongoing work exploring how imaging TCD can provide an estimate of lumen diameter [102], which may allow for an improved

understanding of actual cerebral blood flow and volume. Similar to the other noninvasive devices previously reviewed, further studies are needed to delineate how and when TCD may be incorporated into pediatric critical care and how it may impact clinical decision-making for the betterment of patient outcomes.

### Supplementary Information

The online version contains supplementary material available at <https://doi.org/10.1007/s12028-023-01730-4>.

### Author details

<sup>1</sup> Division of Critical Care Medicine, Department of Pediatrics, Nationwide Children's Hospital and The Ohio State University, Columbus, OH, USA. <sup>2</sup> Division of Pediatric Critical Care, Montreal Children's Hospital and McGill University, Montreal, Canada. <sup>3</sup> Department of Neurology, State University of New York Downstate College of Medicine, Brooklyn, NY, USA. <sup>4</sup> Department of Neurology, Boston Children's Hospital and Harvard Medical School, Boston, MA, USA.

### Author contributions

All authors are responsible for the reported research. All authors participated in the concept and design, analysis and interpretation of data, and drafting or revising of the manuscript for intellectual content, and all authors approved the final manuscript as submitted.

### Source of support

This study was not funded.

### Conflict of interest

Dr. LaRovere has a patent pending for emboli detection methods.

### Ethical approval/informed consent

This study adheres to ethical guidelines. Patient consent was not necessary after ethics committee approval because solely retrospective data were obtained and patients were anonymized.

### Publisher's Note

Springer Nature remains neutral with regard to jurisdictional claims in published maps and institutional affiliations.

Springer Nature or its licensor (e.g. a society or other partner) holds exclusive rights to this article under a publishing agreement with the author(s) or other rightsholder(s); author self-archiving of the accepted manuscript version of this article is solely governed by the terms of such publishing agreement and applicable law.

Received: 20 May 2022 Accepted: 3 April 2023

Published: 9 May 2023

### References

1. Kirschen MP, LaRovere K, Balakrishnan B, et al. A survey of neuromonitoring practices in north American pediatric intensive care units. *Pediatr Neurol.* 2022;126:125–30. <https://doi.org/10.1016/j.pediatrneurol.2021.11.002>.
2. Brown KL, Agrawal S, Kirschen MP, et al. The brain in pediatric critical care: unique aspects of assessment, monitoring, investigations, and follow-up. *Intensive Care Med.* 2022;48(5):535–47. <https://doi.org/10.1007/s00134-022-06683-4>.
3. Hall CA, Chilcott RP. Eyeing up the future of the pupillary light reflex in neurodiagnostics. *Diagnostics (Basel).* 2018. <https://doi.org/10.3390/diagnostics8010019>.
4. Bower MM, Sweidan AJ, Xu JC, Stern-Neze S, Yu W, Groysman LI. Quantitative pupillometry in the intensive care unit. *J Intensive Care Med.* 2021;36(4):383–91. <https://doi.org/10.1177/0885066619881124>.

5. Belliveau AP, Somani AN, Dossani RH. Pupillary light reflex. Treasure Island: StatPearls; 2022.
6. Opic P, Ruegg S, Marsch S, Gut SS, Sutter R. Automated quantitative pupillometry in the critically ill: a systematic review of the literature. *Neurology*. 2021;97(6):e629–42. <https://doi.org/10.1212/WNL.00000000000012295>.
7. Lussier BL, Olson DM, Aiyagari V. Automated pupillometry in neurocritical care: research and practice. *Curr Neurol Neurosci Rep*. 2019;19(10):71. <https://doi.org/10.1007/s11910-019-0994-z>.
8. Couret D, Boumaza D, Grisotto C, et al. Reliability of standard pupillometry practice in neurocritical care: an observational, double-blinded study. *Crit Care*. 2016;20:99. <https://doi.org/10.1186/s13054-016-1239-z>.
9. Meeker M, Du R, Bacchetti P, et al. Pupil examination: validity and clinical utility of an automated pupillometer. *J Neurosci Nurs*. 2005;37(1):34–40.
10. Olson DM, Stutzman S, Saju C, Wilson M, Zhao W, Aiyagari V. Interrater reliability of pupillary assessments. *Neurocrit Care*. 2016;24(2):251–7. <https://doi.org/10.1007/s12028-015-0182-1>.
11. Robba C, Moro Salihovic B, Pozzebon S, et al. Comparison of 2 automated pupillometry devices in critically ill patients. *J Neurosurg Anesthesiol*. 2020;32(4):323–9. <https://doi.org/10.1097/ANA.0000000000000604>.
12. Boev AN, Fountas KN, Karamelas I, et al. Quantitative pupillometry: normative data in healthy pediatric volunteers. *J Neurosurg*. 2005;103(6 Suppl):496–500. <https://doi.org/10.3171/ped.2005.103.6.0496>.
13. Shah SS, Ranaivo HR, Mets-Halgrimson RB, Rychlik K, Kurup SP. Establishing a normative database for quantitative pupillometry in the pediatric population. *BMC Ophthalmol*. 2020;20(1):121. <https://doi.org/10.1186/s12886-020-01389-x>.
14. Chen JW, Gombart ZJ, Rogers S, Gardiner SK, Cecil S, Bullock RM. Pupillary reactivity as an early indicator of increased intracranial pressure: the introduction of the Neurological Pupil index. *Surg Neurol Int*. 2011;2:82. <https://doi.org/10.4103/2152-7806.82248>.
15. Zafar SF, Suarez JL. Automated pupillometer for monitoring the critically ill patient: a critical appraisal. *J Crit Care*. 2014;29(4):599–603. <https://doi.org/10.1016/j.jccr.2014.01.012>.
16. Tran DK, Poole C, Tobias E, Moores L, Espinoza M, Chen JW. 7-Year experience with automated pupillometry and direct integration with the hospital electronic medical record. *World Neurosurg*. 2022. <https://doi.org/10.1016/j.wneu.2022.01.022>.
17. Larson MD, Singh V. Portable infrared pupillometry in critical care. *Crit Care*. 2016;20(1):161. <https://doi.org/10.1186/s13054-016-1349-7>.
18. Aoun SG, Stutzman SE, Vo PN, et al. Detection of delayed cerebral ischemia using objective pupillometry in patients with aneurysmal subarachnoid hemorrhage. *J Neurosurg*. 2019;132(1):27–32. <https://doi.org/10.3171/2018.9.JNS181928>.
19. Solari D, Rossetti AO, Carteron L, et al. Early prediction of coma recovery after cardiac arrest with blinded pupillometry. *Ann Neurol*. 2017;81(6):804–10. <https://doi.org/10.1002/ana.24943>.
20. Oddo M, Sandroni C, Citerio G, et al. Quantitative versus standard pupillary light reflex for early prognostication in comatose cardiac arrest patients: an international prospective multicenter double-blinded study. *Intensive Care Med*. 2018;44(12):2102–11. <https://doi.org/10.1007/s00134-018-5448-6>.
21. Freeman AD, McCracken CE, Stockwell JA. Automated pupillary measurements inversely correlate with increased intracranial pressure in pediatric patients with acute brain injury or encephalopathy. *Pediatr Crit Care Med*. 2020;21(8):753–9. <https://doi.org/10.1097/PCC.0000000000000327>.
22. Greer DM, Shemie SD, Lewis A, et al. Determination of brain death/death by neurologic criteria: the world brain death project. *JAMA*. 2020;324(11):1078–97. <https://doi.org/10.1001/jama.2020.11586>.
23. Hanning CD, Alexander-Williams JM. Pulse oximetry: a practical review. *BMJ*. 1995;311(7001):367–70. <https://doi.org/10.1136/bmj.311.7001.367>.
24. Jobsis FF. Non-invasive, infra-red monitoring of cerebral O<sub>2</sub> sufficiency, bloodvolume, HbO<sub>2</sub>-Hb shifts and bloodflow. *Acta Neurol Scand Suppl*. 1977;64:452–3.
25. Jarrett CL, Shields KL, Broxterman RM, et al. Imaging transcranial Doppler ultrasound to measure middle cerebral artery blood flow: the importance of measuring vessel diameter. *Am J Physiol Regul Integr Comp Physiol*. 2020;319(1):R33–r42. <https://doi.org/10.1152/ajpregu.00025.2020>.
26. Denault AY, Shaaban-Ali M, Cournoyer A, Benkreira A, Mailhot T. Chapter 7—Near-infrared spectroscopy. In: Prabhakar H, editor. *Neuromonitoring techniques*. Academic Press; 2018. p. 179–233.
27. Shaaban-Ali M, Momeni M, Denault A. Clinical and technical limitations of cerebral and somatic near-infrared spectroscopy as an oxygenation monitor. *J Cardiothorac Vasc Anesth*. 2021;35(3):763–79. <https://doi.org/10.1053/j.jvca.2020.04.054>.
28. Weiss M, Dullenkopf A, Kolarova A, Schulz G, Frey B, Baenziger O. Near-infrared spectroscopic cerebral oxygenation reading in neonates and infants is associated with central venous oxygen saturation. *Paediatr Anaesth*. 2005;15(2):102–9. <https://doi.org/10.1111/j.1460-9592.2005.01404.x>.
29. Nagdyman N, Fleck T, Schubert S, et al. Comparison between cerebral tissue oxygenation index measured by near-infrared spectroscopy and venous jugular bulb saturation in children. *Intensive Care Med*. 2005;31(6):846–50. <https://doi.org/10.1007/s00134-005-2618-0>.
30. Nagdyman N, Ewert P, Peters B, Miera O, Fleck T, Berger F. Comparison of different near-infrared spectroscopic cerebral oxygenation indices with central venous and jugular venous oxygenation saturation in children. *Pediatr Anesth*. 2008;18(2):160–6. <https://doi.org/10.1111/j.1460-9592.2007.02365.x>.
31. Abdul-Khaliq H, Troitzsch D, Berger F, Lange PE. Regional transcranial oximetry with near infrared spectroscopy (NIRS) in comparison with measuring oxygen saturation in the jugular bulb in infants and children for monitoring cerebral oxygenation. *Biomed Tech (Berl)*. 2000;45(11):328–32. <https://doi.org/10.1515/bmte.2000.45.11.328>.
32. Abdul-Khaliq H, Schubert S, Troitzsch D, et al. Dynamic changes in cerebral oxygenation related to deep hypothermia and circulatory arrest evaluated by near-infrared spectroscopy. *Acta Anaesthesiol Scand*. 2001;45(6):696–701. <https://doi.org/10.1034/j.1399-6576.2001.045006696.x>.
33. Abdul-Khaliq H, Troitzsch D, Schubert S, et al. Cerebral oxygen monitoring during neonatal cardiopulmonary bypass and deep hypothermic circulatory arrest. *Thorac Cardiovasc Surg*. 2002;50(2):77–81. <https://doi.org/10.1055/s-2002-26698>.
34. Kim MB, Ward DS, Cartwright CR, Kolano J, Chlebowski S, Henson LC. Estimation of jugular venous O<sub>2</sub> saturation from cerebral oximetry or arterial O<sub>2</sub> saturation during isocapnic hypoxia. *J Clin Monit Comput*. 2000;16(3):191–9. <https://doi.org/10.1023/a:1009940031063>.
35. Cho H, Nemoto EM, Sanders M, Fernandez K, Yonas H. Comparison of two commercially available near-infrared spectroscopy instruments for cerebral oximetry. Technical note *J Neurosurg*. 2000;93(2):351–4. <https://doi.org/10.3171/jns.2000.93.2.0351>.
36. Dix LM, van Bel F, Baerts W, Lemmers PM. Comparing near-infrared spectroscopy devices and their sensors for monitoring regional cerebral oxygen saturation in the neonate. *Pediatr Res*. 2013;74(5):557–63. <https://doi.org/10.1038/pr.2013.133>.
37. Grubhofer G, Tonninger W, Keznickl P, et al. A comparison of the monitors INVOS 3100 and NIRO 500 in detecting changes in cerebral oxygenation. *Acta Anaesthesiol Scand*. 1999;43(4):470–5. <https://doi.org/10.1034/j.1399-6576.1999.430417.x>.
38. Hessel TW, Hyttel-Sorensen S, Greisen G. Cerebral oxygenation after birth—a comparison of INVOS(R) and FORE-SIGHT near-infrared spectroscopy oximeters. *Acta Paediatr*. 2014;103(5):488–93. <https://doi.org/10.1111/apa.12567>.
39. Hyttel-Sorensen S, Kleiser S, Wolf M, Greisen G. Calibration of a prototype NIRS oximeter against two commercial devices on a blood-lipid phantom. *Biomed Opt Express*. 2013;4(9):1662–72. <https://doi.org/10.1364/BOE.4.001662>.
40. Watzman HM, Kurth CD, Montenegro LM, Rome J, Steven JM, Nicolson SC. Arterial and venous contributions to near-infrared cerebral oximetry. *Anesthesiology*. 2000;93(4):947–53. <https://doi.org/10.1097/0000542-200010000-00012>.
41. Ito H, Ibaraki M, Kanno I, Fukuda H, Miura S. Changes in the arterial fraction of human cerebral blood volume during hypercapnia and hypocapnia measured by positron emission tomography. *J Cereb Blood Flow Metab*. 2005;25(7):852–7. <https://doi.org/10.1038/sj.jcbfm.9600076>.
42. Schober A, Feiner JR, Bickler PE, Rollins MD. Effects of changes in arterial carbon dioxide and oxygen partial pressures on cerebral oximeter performance. *Anesthesiology*. 2018;128(1):97–108. <https://doi.org/10.1097/ALN.0000000000001898>.

43. Namekawa M, Ishida K, Kimura M, Fujii C, Yamashita S. Alkaptonuric ochronosis and the failure of regional cerebral tissue oxygen saturation monitoring by two different near-infrared spectroscopy devices. *J Cardiothorac Vasc Anesth*. 2018;32(5):2286–8. <https://doi.org/10.1053/j.jvca.2017.12.046>.
44. Bickler PE, Feiner JR, Rollins MD. Factors affecting the performance of 5 cerebral oximeters during hypoxia in healthy volunteers. *Anesth Analg*. 2013;117(4):813–23. <https://doi.org/10.1213/ANE.0b013e31829d763>.
45. Kurth CD, Steven JL, Montenegro LM, et al. Cerebral oxygen saturation before congenital heart surgery. *Ann Thorac Surg*. 2001;72(1):187–92. [https://doi.org/10.1016/s0003-4975\(01\)02632-7](https://doi.org/10.1016/s0003-4975(01)02632-7).
46. Bernal NP, Hoffman GM, Ghanayem NS, Arca MJ. Cerebral and somatic near-infrared spectroscopy in normal newborns. *J Pediatr Surg*. 2010;45(6):1306–10. <https://doi.org/10.1016/j.jpedsurg.2010.02.110>.
47. Chan MJ, Chung T, Glassford NJ, Bellomo R. Near-infrared spectroscopy in adult cardiac surgery patients: a systematic review and meta-analysis. *J Cardiothorac Vasc Anesth*. 2017;31(4):1155–65. <https://doi.org/10.1053/j.jvca.2017.02.187>.
48. Alderliesten T, Dix L, Baerts W, et al. Reference values of regional cerebral oxygen saturation during the first 3 days of life in preterm neonates. *Pediatr Res*. 2016;79(1–1):55–64. <https://doi.org/10.1038/pr.2015.186>.
49. Kurth CD, Levy WJ, McCann J. Near-infrared spectroscopy cerebral oxygen saturation thresholds for hypoxia-ischemia in piglets. *J Cereb Blood Flow Metab*. 2002;22(3):335–41. <https://doi.org/10.1097/00004647-200203000-00011>.
50. Hyttel-Sorensen S, Greisen G, Als-Nielsen B, Gluud C. Cerebral near-infrared spectroscopy monitoring for prevention of brain injury in very preterm infants. *Cochrane Database Syst Rev*. 2017;9(9):CD011506. <https://doi.org/10.1002/14651858.CD011506.pub2>.
51. Hirsch JC, Charpie JR, Ohye RG, Gurney JG. Near-infrared spectroscopy: what we know and what we need to know—a systematic review of the congenital heart disease literature. *J Thoracic Cardiovasc Surg*. 2009;137(1):154–9, 159e1–12. <https://doi.org/10.1016/j.jtcvs.2008.08.005>.
52. Kampfl A, Pfausler B, Denchev D, Jaring HP, Schmutzhard E. Near infrared spectroscopy (NIRS) in patients with severe brain injury and elevated intracranial pressure. A pilot study. *Acta Neurochir Suppl*. 1997;70:112–4. [https://doi.org/10.1007/978-3-7091-6837-0\\_35](https://doi.org/10.1007/978-3-7091-6837-0_35).
53. Kirkpatrick PJ, Smielewski P, Czosnyka M, Menon DK, Pickard JD. Near-infrared spectroscopy use in patients with head injury. *J Neurosurg*. 1995;83(6):963–70. <https://doi.org/10.3171/jns.1995.83.6.0963>.
54. Lang SS, Khanna O, Atkin NJ, et al. Perioperative near-infrared spectroscopy cerebral oxygen saturation in symptomatic pediatric hydrocephalus patients at risk for intracranial hypertension. *J Neurosurg Pediatr*. 2019. <https://doi.org/10.3171/2019.9.Peds19457>.
55. Zuluaga MT, Esch ME, Cviljanovich NZ, Gupta N, McQuillen PS. Diagnosis influences response of cerebral near infrared spectroscopy to intracranial hypertension in children. *Pediatr Crit Care Med*. 2010;11(4):514–22. <https://doi.org/10.1097/PCC.0b013e3181c51cf1>.
56. Ghalenoui H, Saidi H, Azar M, Yahyavi ST, Borghei Razavi H, Khalatbari M. Near-infrared laser spectroscopy as a screening tool for detecting hematoma in patients with head trauma. *Prehosp Disaster Med*. 2008;23(6):558–61. <https://doi.org/10.1017/s1049023x00006415>.
57. Kahraman S, Kayali H, Atabey C, Acar F, Gocmen S. The accuracy of near-infrared spectroscopy in detection of subdural and epidural hematomas. *J Trauma*. 2006;61(6):1480–3. <https://doi.org/10.1097/01.ta.00000197616.10279.48>.
58. Kessel B, Jeroukhimov I, Ashkenazi I, et al. Early detection of life-threatening intracranial haemorrhage using a portable near-infrared spectroscopy device. *Injury*. 2007;38(9):1065–8. <https://doi.org/10.1016/j.injury.2007.05.009>.
59. Bressan S, Daverio M, Martinolli F, et al. The use of handheld near-infrared device (Infrascanner) for detecting intracranial haemorrhages in children with minor head injury. *Childs Nerv Syst*. 2014;30(3):477–84. <https://doi.org/10.1007/s00381-014-2368-9>.
60. Lewartowska-Nyga D, Nyga K, Skotnicka-Klonowicz G. Can infrascanner be useful in hospital emergency departments for diagnosing minor head injury in children? *Dev Period Med*. 2017;21(1):51–9. <https://doi.org/10.34763/devperiodmed.20172101.5159>.
61. Kirschen MP, Myers SR, Neuman MI, et al. Intracranial traumatic hematoma detection in children using a portable near-infrared spectroscopy device. *West J Emerg Med*. 2021;22(3):782–91. <https://doi.org/10.5811/westjem.2020.11.47251>.
62. Salonia R, Bell MJ, Kochanek PM, Berger RP. The utility of near infrared spectroscopy in detecting intracranial hemorrhage in children. *J Neurotrauma*. 2012;29(6):1047–53. <https://doi.org/10.1089/neu.2011.1890>.
63. Ito N, Nishiyama K, Callaway CW, et al. Noninvasive regional cerebral oxygen saturation for neurological prognostication of patients with out-of-hospital cardiac arrest: a prospective multicenter observational study. *Resuscitation*. 2014;85(6):778–84. <https://doi.org/10.1016/j.resuscitation.2014.02.012>.
64. Parnia S, Yang J, Nguyen R, et al. Cerebral oximetry during cardiac arrest: a multicenter study of neurologic outcomes and survival\*. *Crit Care Med*. 2016;44(9):1663–74. <https://doi.org/10.1097/CCM.0000000000001723>.
65. Singer AJ, Ahn A, Inigo-Santiago LA, Thode HC, Henry MC, Parnia S. Cerebral oximetry levels during CPR are associated with return of spontaneous circulation following cardiac arrest: an observational study. *Emerg Med J*. 2015;32(5):353–6. <https://doi.org/10.1136/emerm-2013-203467>.
66. Abramo T, Aggarwal N, Kane I, Crossman K, Meredith M. Cerebral oximetry and cerebral blood flow monitoring in 2 pediatric survivors with out-of-hospital cardiac arrest. *Am J Emerg Med*. 2014;32(4):394.e5–394.e10. <https://doi.org/10.1016/j.ajem.2013.10.039>.
67. Abramo TJ, Meredith M, Jaeger M, et al. Cerebral oximetry with blood volume index in asystolic pediatric cerebrospinal fluid malfunctioning shunt patients. *Am J Emerg Med*. 2014;32(11):1439.e1–1439.e7. <https://doi.org/10.1016/j.ajem.2014.04.007>.
68. Caglar A, Er A, Ulusoy E, et al. Cerebral oxygen saturation monitoring in pediatric cardiopulmonary resuscitation patients in the emergency settings: a small descriptive study. *Turk J Pediatr*. 2017;59(6):642–7. <https://doi.org/10.24953/turkjped.2017.06.004>.
69. Francoeur C, Landis WP, Winters M, et al. Near-infrared spectroscopy during cardiopulmonary resuscitation for pediatric cardiac arrest: a prospective, observational study. *Resuscitation*. 2022;174:35–41. <https://doi.org/10.1016/j.resuscitation.2022.03.014>.
70. Rivera-Lara L, Geocadin R, Zorrilla-Vaca A, et al. Validation of near-infrared spectroscopy for monitoring cerebral autoregulation in comatose patients. *Neurocrit Care*. 2017;27(3):362–9. <https://doi.org/10.1007/s12028-017-0421-8>.
71. Sekhon MS, Smielewski P, Bhat TD, et al. Using the relationship between brain tissue regional saturation of oxygen and mean arterial pressure to determine the optimal mean arterial pressure in patients following cardiac arrest: a pilot proof-of-concept study. *Resuscitation*. 2016;106:120–5. <https://doi.org/10.1016/j.resuscitation.2016.05.019>.
72. Kirschen MP, Majmudar T, Beaulieu F, et al. Deviations from NIRS-derived optimal blood pressure are associated with worse outcomes after pediatric cardiac arrest. *Resuscitation*. 2021;168:110–8. <https://doi.org/10.1016/j.resuscitation.2021.09.023>.
73. Lee JK, Brady KM, Chung S-E, et al. A pilot study of cerebrovascular reactivity autoregulation after pediatric cardiac arrest. *Resuscitation*. 2014;85(10):1387–93. <https://doi.org/10.1016/j.resuscitation.2014.07.006>.
74. Denault A, Deschamps A, Murkin JM. A proposed algorithm for the intraoperative use of cerebral near-infrared spectroscopy. *Semin Cardiothorac Vasc Anesth*. 2007;11(4):274–81. <https://doi.org/10.1177/1089253207311685>.
75. Trafidlo T, Gaszyński T, Gaszyński W, Nowakowska-Domagala K. Intraoperative monitoring of cerebral NIRS oximetry leads to better postoperative cognitive performance: a pilot study. *Int J Surg (London, England)*. 2015. <https://doi.org/10.1016/j.ijsu.2015.02.009>.
76. Afshari A, Saager R, Zhou X, et al. Skin pigmentation impact on cerebral oximetry: Development and implementation of a phantom-based test method (Conference Presentation): SPIE, 2019.
77. Sun X, Ellis J, Corso PJ, Hill PC, Chen F, Lindsay J. Skin pigmentation interferes with the clinical measurement of regional cerebral oxygen saturation. *Br J Anaesth*. 2015;114(2):276–80. <https://doi.org/10.1093/bja/aeu335>.
78. de Courson H, Proust-Lima C, Tuaz E, Georges D, Verchere E, Biais M. Relationship between brain tissue oxygen and near-infrared spectroscopy in patients with nontraumatic subarachnoid



- hemorrhage. *Neurocrit Care*. 2022;37(3):620–8. <https://doi.org/10.1007/s12028-022-01563-7>.
79. Roldan M, Kyriacou PA. Near-infrared spectroscopy (NIRS) in traumatic brain injury (TBI). *Sensors (Basel)*. 2021. <https://doi.org/10.3390/s21051586>.
  80. Davies DJ, Clancy M, Dehghani H, et al. Cerebral oxygenation in traumatic brain injury: can a non-invasive frequency domain near-infrared spectroscopy device detect changes in brain tissue oxygen tension as well as the established invasive monitor? *J Neurotrauma*. 2019;36(7):1175–83. <https://doi.org/10.1089/neu.2018.5667>.
  81. Leal-Naval SR, Cayuela A, Arellano-Orden V, et al. Invasive and non-invasive assessment of cerebral oxygenation in patients with severe traumatic brain injury. *Intensive Care Med*. 2010;36(8):1309–17. <https://doi.org/10.1007/s00134-010-1920-7>.
  82. Forcione M, Ganau M, Prisco L, et al. Mismatch between tissue partial oxygen pressure and near-infrared spectroscopy neuromonitoring of tissue respiration in acute brain trauma: the rationale for implementing a multimodal monitoring strategy. *Int J Mol Sci*. 2021. <https://doi.org/10.3390/ijms22031122>.
  83. Aaslid R, Markwalder TM, Nornes H. Noninvasive transcranial Doppler ultrasound recording of flow velocity in basal cerebral arteries. *J Neurosurg*. 1982;57(6):769–74. <https://doi.org/10.3171/jns.1982.57.6.0769>.
  84. Robba C, Cardim D, Sekhon M, Budohoski K, Czosnyka M. Transcranial Doppler: a stethoscope for the brain-neurocritical care use. *J Neurosci Res*. 2018;96(4):720–30. <https://doi.org/10.1002/jnr.24148>.
  85. Neurovascular sonography. In: Wendy C. Ziai CLC, ed.: Springer Nature Switzerland AG; 2022.
  86. Moehring MA, Spencer MP. Power M-mode Doppler (PMD) for observing cerebral blood flow and tracking emboli. *Ultrasound Med Biol*. 2002;28(1):49–57. [https://doi.org/10.1016/s0301-5629\(01\)00486-0](https://doi.org/10.1016/s0301-5629(01)00486-0).
  87. Bang OY, Lee MJ, Ryoo S, Kim SJ, Kim JW. Patent foramen ovale and stroke-current status. *J Stroke*. 2015;17(3):229–37. <https://doi.org/10.5853/jos.2015.17.3.229>.
  88. Stannard B, Levin MA, Lin HM, Weiner MM. Regional cerebral oximetry is consistent across self-reported racial groups and predicts 30-day mortality in cardiac surgery: a retrospective analysis. *J Clin Monit Comput*. 2021;35(2):413–21. <https://doi.org/10.1007/s10877-020-00487-x>.
  89. Couture A, Veyrac C, Baud C, Saguinthaah M, Ferran JL. Advanced cranial ultrasound: transfontanelle Doppler imaging in neonates. *Eur Radiol*. 2001;11(12):2399–410. <https://doi.org/10.1007/s00330-001-1150-z>.
  90. LaRovere KL, O'Brien NF. Transcranial Doppler sonography in pediatric neurocritical care: a review of clinical applications and case illustrations in the pediatric intensive care unit. *J Ultrasound Med*. 2015;34(12):2121–32. <https://doi.org/10.7863/ultra.15.02016>.
  91. Mejia LLP, Ergin BB, Rivera LL, et al. Neuro-ICU: cerebral hemodynamics and transcranial Doppler (TCD/TCCS) waveform interpretation in the most common neurocritical pathologies. In: Rodríguez CN, Baracchini C, Mejia-Mantilla JH, et al., editors. *Neurosonology in critical care: monitoring the neurological impact of the critical pathology*. Cham: Springer; 2022. p. 299–318.
  92. Kashif FM, Verghese GC, Novak V, Czosnyka M, Heldt T. Model-based noninvasive estimation of intracranial pressure from cerebral blood flow velocity and arterial pressure. *Sci Transl Med*. 2012;4(129):129–44. <https://doi.org/10.1126/scitranslmed.3003249>.
  93. Fanelli A, Vonberg FW, LaRovere KL, et al. Fully automated, real-time, calibration-free, continuous noninvasive estimation of intracranial pressure in children. *J Neurosurg Pediatr*. 2019. <https://doi.org/10.3171/2019.5.PEDS19178>.
  94. Puppo C, et al. Neurosonology in the ICU: transcranial Doppler (TCD) protocol. In: Rodríguez CN, Baracchini C, Mejia-Mantilla JH, et al., editors. *Neurosonology in critical care: monitoring the neurological impact of the critical pathology*. Cham: Springer; 2022. p. 215–32.
  95. O'Brien NF, Reuter-Rice K, Wainwright MS, et al. Practice recommendations for transcranial doppler ultrasonography in critically ill children in the pediatric intensive care unit: a multidisciplinary expert consensus statement. *J Pediatr Intensive Care*. 2021;10(2):133–42. <https://doi.org/10.1055/s-0040-1715128>.
  96. Rodríguez CN, Pugin D, et al. Neurosonology in ICU: transcranial color-coded duplex sonography (TCCS) protocol. In: Rodríguez CN, Baracchini C, Mejia-Mantilla JH, et al., editors. *Neurosonology in critical care: monitoring the neurological impact of the critical pathology*. Cham: Springer; 2022. p. 251–81.
  97. Appavu B, Burrows BT, Nickoles T, et al. Implementation of multimodality neurologic monitoring reporting in pediatric traumatic brain injury management. *Neurocrit Care*. 2021;35(1):3–15. <https://doi.org/10.1007/s12028-021-01190-8>.
  98. LaRovere KL, Tasker RC, Wainwright M, et al. Transcranial Doppler ultrasound during critical illness in children: survey of practices in pediatric neurocritical care centers. *Pediatric Crit Care Med*. 2020;21(1):67–74. <https://doi.org/10.1097/PCC.0000000000002118>.
  99. Lin JJ, Kuo HC, Hsia SH, et al. The utility of a point-of-care transcranial Doppler ultrasound management algorithm on outcomes in pediatric asphyxial out-of-hospital cardiac arrest - an exploratory investigation. *Front Med (Lausanne)*. 2021;8:690405. <https://doi.org/10.3389/fmed.2021.690405>.
  100. Fonseca Y, Tshimanga T, Ray S, et al. Transcranial Doppler ultrasonographic evaluation of cerebrovascular abnormalities in children with acute bacterial meningitis. *Front Neurol*. 2020;11:558857. <https://doi.org/10.3389/fneur.2020.558857>.
  101. Evans DH, et al. Transcranial Doppler ultrasound: physical principles. In: Rodríguez CN, Baracchini C, Mejia-Mantilla JH, et al., editors. *Neurosonology in critical care: monitoring the neurological impact of the critical pathology*. Cham: Springer; 2022. p. 99–116.
  102. Minhas PS, Menon DK, Smielewski P, et al. Positron emission tomographic cerebral perfusion disturbances and transcranial Doppler findings among patients with neurological deterioration after subarachnoid hemorrhage. *Neurosurgery* 2003;52(5):1017–22; discussion 1022–4. <https://www.ncbi.nlm.nih.gov/pubmed/12699542>.
  103. Sentenac P, Charbit J, Maury C, et al. The frontal bone window for transcranial Doppler ultrasonography in critically ill patients: validation of a new approach in the ICU. *Neurocrit Care*. 2020;33(1):115–23. <https://doi.org/10.1007/s12028-019-00869-3>.